J. Biochem. **140**, 535–542 (2006)
doi:10.1093/jb/mvj183

Crystal Structure of TTHA0252 from *Thermus thermophilus* HB8, a RNA Degradation Protein of the Metallo-β-lactamase Superfamily

Hirohito Ishikawa[1], Noriko Nakagawa[1,2], Seiki Kuramitsu[1,2] and Ryoji Masui[1,2,*]
[1]Department of Biological Sciences, Graduate School of Science, Osaka University, Toyonaka, Osaka 560-0043; and [2]RIKEN Harima Institute at SPring-8, 1-1-1 Kouto, Sayo-cho, Sayo, Hyogo 113-0033

Received April 27, 2006; accepted August 22, 2006

In bacterial RNA metabolism, mRNA degradation is an important process for gene expression. Recently, a novel ribonuclease (RNase), belonging to the β-CASP family within the metallo-β-lactamase superfamily, was identified as a functional homologue of RNase E, a major component for mRNA degradation in *Escherichia coli*. Here, we have determined the crystal structure of TTHA0252 from *Thermus thermophilus* HB8, which represents the first report of the tertiary structure of a β-CASP family protein. TTHA0252 comprises two separate domains: a metallo-β-lactamase domain and a "clamp" domain. The active site of the enzyme is located in a cleft between the two domains, which includes two zinc ions coordinated by seven conserved residues. Although this configuration is similar to those of other β-lactamases, TTHA0252 has one conserved His residue characteristic of the β-CASP family as a ligand. We also detected nuclease activity of TTHA0252 against rRNAs of *T. thermophilus*. Our results reveal structural and functional aspects of novel RNase E–like enzymes with a β-CASP fold.

Key words: β-CASP, crystal structure, metallo-β-lactamase superfamily, RNase, *Thermus thermophilus*.

Abbreviations: CD, circular dichroism; dsDNA, double-stranded DNA; PAR, 4-(2-pyridylazo)resorcinol; SAD, single-wavelength anomalous dispersion; SeMet, selenomethionine; TBE, Tris-borate-EDTA; XAFS, X-ray absorption fine structure spectroscopy.

All cells synthesize a diverse variety of RNAs from DNA or RNA. The unique shape of RNA molecules allows them to perform specific cellular roles (*1*). For example, mRNAs act as templates for protein synthesis, rRNAs are the main structural and catalytic components of the ribosome and tRNAs are the adaptor molecules that match amino acids to their cognate codon(s) in the mRNA. In addition to these ubiquitous RNAs, there are a variety of other functional RNAs in the cell. Together, these RNA species and their interacting proteins constitute RNA metabolism within the cell.

The degradation of mRNA is an important step in regulating the intracellular level of RNA species (*2*). This active process is executed by ribonucleases (RNases) in conjunction with several other proteins. In *Escherichia coli*, ribonucleolytic machinery, termed the RNA degradosome, participates in mRNA degradation and RNA processing (*3*). RNase E, a major component of the degradosome, initially cleaves mRNA endonucleolytically and is essential for cell viability (*4*). Although mRNA degradation is considered to be a common mechanism in bacterial RNA metabolism, many bacteria have no homologue of *E. coli* RNase E.

Recently, it was reported that two endoribonucleases, RNases J1 and J2 from *Bacillus subtilis* (originally referred to as YkqC and YmfA, respectively), are functional homologues of *E. coli* RNase E (*5*). These novel RNases belong to the β-CASP family within the metallo-β-lactamase superfamily (*6*). There are four groups, classed A, B, C and D, of β-lactamases, which are involved in resistance against β-lactams. Class A, C and D β-lactamases are serine-utilizing hydrolases, whereas class B enzymes, also called metallo-β-lactamases, utilize a catalytic zinc center instead (*7*). However, the recent accumulation of sequence and structural data has revealed that many relatives of metallo-β-lactamases are distributed among all kingdoms and diverged in their sequences and functions. β-CASP family proteins are characterized by three conserved sequence motifs (A, B and C), following the four typical metallo-β-lactamase motifs (1 to 4), whereas archetypal metallo-β-lactamases have motif 5 immediately after motif 4 (*6*). Motif A has a conserved acidic residue (Asp or Glu) and motif B has a conserved His residue. In motif C, either His or Val is conserved at a particular position. Proteins with the conserved His in motif C are predicted to possess RNA-degrading activity, whereas proteins with the conserved Val possess DNA-degrading activity (*6*). In the Pfam database, motifs B and C are defined as the RNA metabolising metallo-β-lactamase domain (RMMBL).

Although it is known that at least two β-CASP enzymes from *B. subtilis*, RNases J1 and J2 possess RNA nuclease activity, the mechanism of action of these protein family members remains unclear. Since homologues of RNases J1 and J2 are found in many eubacteria and archaea, unraveling the molecular and cellular mechanism of these putative RNases is crucial to understanding RNA metabolism in organisms that lack RNase E. To address this issue, an

*To whom correspondence should be addressed at: Department of Biology, Graduate School of Science, Osaka University, 1-1 Machikaneyama-cho, Toyonaka, Osaka 560-0043. Tel: +81-6-6850-5434, Fax: +81-6-6850-5442, E-mail: rmasui@bio.sci.osaka-u.ac.jp

approach based on three-dimensional structural information is essential. The crystal structure of RNase Z, an RNase belonging to the metallo-β-lactamase superfamily, from both *B. subtilis* (*8*, *9*) and *Thermotoga maritima* (*10*) has been solved. However, no structure of a β-CASP family member has previously been determined.

In this paper, we solved the crystal structure of TTHA0252, a β-CASP family protein of *Thermus thermophilus*. The thermostable properties of proteins from *T. thermophilus* HB8 make them particularly suitable for structural and functional analyses (*11*, *12*). We also show that THA0252 possesses nuclease activity against RNA. From these results a functional role of the RMMBL motif and a reaction mechanism of β-CASP–type RNases are proposed.

EXPERIMENTAL PROCEDURES

Cloning and Overproduction—Sequence analysis of the *T. thermophilus* HB8 genome (DDBJ/EMBL/GeneBank AB107660) identified two ORFs encoding proteins homologous to β-CASP family members. Using this sequence information, we synthesized two primers for amplification of one of the target genes (TTHA0252, project code 1672) by the polymerase chain reaction. Amplification was performed by standard protocols (*13*) and the amplified gene fragment was ligated into pT7Blue (Novagen, Madison, WI) by TA cloning and confirmed by sequencing. Using the *Nde*I and *Bgl*II sites, the fragment bearing the target gene was ligated into pET-11a (Novagen). The resultant expression plasmid pET-11a/ttha0252 was used to transform *E. coli* BL21(DE3) (Novagen). The transformant was cultured at 37°C in 1.5 liter LB medium containing ampicillin (50 μg ml^{-1}) overnight and cells were harvested by centrifugation and stored at –20°C. The selenomethionine (SeMet) derivative of the protein was generated using the methionine auxotroph *E. coli* B834(DE3) as host for the expression plasmid and grown in LeMaster medium (*14*) containing SeMet and lactose. Purification of the SeMet derivative was performed in essentially the same way as the native protein.

Protein Purification—All the following procedures were performed at room temperature unless stated otherwise. Frozen cells were thawed, suspended in 20 mM Tris-HCl (pH 8.0) and 50 mM NaCl and then disrupted by sonication. The lysate was incubated at 70°C for 10 min and ultracentrifuged (200,000 × *g*) for 60 min at 4°C. Ammonium sulfate was added to the resulting supernatant to a final concentration of 1.5 M. The clarified solution was loaded onto a Toyopearl Ether-650 M column (Tosoh, Tokyo, Japan), or a Resource ISO (GE Healthcare Bioscience, Amersham, UK) column for the SeMet derivative, equilibrated with 50 mM sodium phosphate buffer (pH 7.0) and 1.5 M ammonium sulfate. Proteins were eluted with a linear gradient of 1.5–0 M ammonium sulfate. The fractions containing TTHA0252 were loaded onto a Resource Q column (GE Healthcare Bioscience) equilibrated with 20 mM Tris-HCl (pH 8.0) and eluted with a linear gradient of 0–1 M NaCl. Among the fraction containing the target protein, the fractions with the lowest absorbance at 260 nm were applied to HiLoad 16/60 Superdex 200 pg column equilibrated with 20 mM Tris-HCl (pH 8.0) and 0.15 M NaCl. In the case of SeMet derivative, protein fractions were applied to hydroxyapatite CHT2 column (Bio-Rad, Hercules, CA) equilibrated with 10 mM sodium phosphate buffer (pH 7.0) and 1 M NaCl. The target protein was recovered in the flow-through fraction and applied to gel filtration chromatography. The fractions containing TTHA0252 were concentrated and stored at 4°C. At each step, the fractions were analyzed by SDS-PAGE. The concentration of the purified protein was determined using a molar absorption coefficient at 280 nm calculated according to a formula of Kuramitsu *et al.* (*15*).

Spectroscopic Analysis—Circular dichroism (CD) spectra in the far-UV region (200 nm to 250 nm) were obtained at 25°C with a Jasco spectropolarimeter, J-720W, using 10 μM enzyme in 50 mM potassium phosphate buffer, pH 7.0. Thermostability was investigated by recording the molar ellipticity at 222 nm from 15°C to 95°C under the same conditions as above. To reveal the presence of zinc ions bound to the protein, X-ray absorption fine structure (XAFS) spectroscopy was performed at SPring-8, BL44B2. The Zn(II) content was determined colorimetrically using 4-(2-pyridylazo)resorcinol (PAR) under denaturing conditions.

Enzyme Assay—For the RNA degradation assay, short RNAs obtained as by-products of the preparation of plasmids from *E. coli* or total RNAs of *T. thermophilus* HB8 were used as substrate. The reaction mixture contained 10 mM Tris-HCl (pH 8.0), 100 mM KCl, metal ions, 5 μM TTHA0252 and substrate RNA. Reaction with the RNA of *T. thermophilus* was performed with 5 mM metal ions at 37°C for 3 h. Reaction with by-product *E. coli* RNA was performed with 5 mM zinc ions for 5 h. The reaction was stopped by addition of 5× loading buffer (5 mM EDTA, 50% glycerol, 0.05% bromophenol blue). The mixture was loaded onto a 0.7% agarose S gel (TaKaRa, Otsu, Japan) containing 0.5× TBE buffer and 10 mg/ml ethidium bromide and electrophoresed. The RNA fragments stained with ethidium bromide were detected with UV light at 254 nm. For the DNA degradation assay, pT7Blue plasmid either untreated (supercoiled DNA) or digested by *Eco*RI at one site (linear DNA) was used as substrate. Assay conditions were the same as those described for the RNA degradation assay.

Crystallization, Data Collection and Structure Determination—Crystals of TTHA0252 were grown by the hanging-drop, vapor-diffusion method. Drops (1 μl) of 11 mg/ml of SeMet derivative solution were mixed with 1 μl of 1.0 M ammonium sulfate, 1% (w/v) polyethylene glycol 3350 and 0.1 M Bis-Tris (pH 5.5), and equilibrated against 0.2 ml of the reservoir solution at 20°C. For data collection, the crystals were loop-mounted in a cryoprotectant solution containing 2.0 M lithium sulfate and then flash-cooled. Native data were collected at 100 K using beamline BL26B1 at SPring-8. Single-wavelength anomalous dispersion (SAD) data were collected on beamline BL44B2 at SPring-8 at the selenium peak (0.9788 Å). The data were processed with the program package HKL2000 (*16*) and the CCP4 suite (*17*). Selenium sites were determined with the program SOLVE (*18*) using the SAD data sets. The resulting phases were improved with the program RESOLVE (*19*). The model was refined by energy minimization and *B*-factor refinement procedures using Xfit (*20*) and the program package CNS (*21*). SAD data for Zn were also collected on beamline BL44B2 at SPring-8 at the zinc

Table 1. **Summary of data-collection and refinement statistics.**[a]

Data collection statistics	
X-ray source	SPring-8, BL44B2
Wavelength (Å)	0.97882
Temperature (K)	100
Resolution (Å)	2.8 (2.90–2.80)
Space group	*C*2
Unit-cell parameters (Å)	a = 143.2, b = 147.1, c = 121.2, β = 109.249
R_{merge} (%)[b]	6.4 (30.6)
I/σ (I)	53.2 (10.0)
Number of observed reflections	871,724
Number of unique reflections	58,051
Completeness (%)	99.5 (100)
Refinement statistics	
Resolution (Å)	50–2.8
R-factor (%)[c]	24.2
R-free-factor (%)[d]	28.5
rmsd (bond distance) (Å)	0.0095
rmsd (bond angle) (deg.)	1.7
Average B value (Å^2)	68.8
Ramachandran plot	
Most favored region (%)	77.8
Additionally allowed regions (%)	18.8
Generously allowed regions (%)	2.1
Disallowed regions (%)	1.3

[a]The values for the highest resolution shell (2.90–2.80 Å) are given in parentheses. [b]$R_{merge} = \Sigma|I_{obs} - \langle I \rangle| / \Sigma I_{obs}$. [c]$R$-factor = $\Sigma||F_{obs}| - |F_{calc}|| / \Sigma|F_{calc}|$. [d]$R$-free-factor was calculated using 10% of the data.

peak (1.2826 Å) and the zinc-binding sites were identified using an anomalous difference Fourier map. Data collection and refinement statistics are summarized in Table 1.

Figures were drawn using the programs PyMol (DeLano Scientific). The atomic coordinates and structure factors have been deposited in the Protein Data Bank with the PDB ID code of 2DKF.

RESULTS

Sequence Analysis—Our analysis of the *T. thermophilus* HB8 genome sequence identified two ORFs, TTHA0252 and TTHA1140, belonging to the β-CASP family among nine ORFs containing the metallo-β-lactamase fold motif. A sequence alignment of TTHA0252 and proteins previously identified as β-CASP family proteins is shown in Fig. 1. TTHA0252, consisting of 431 amino acid residues, contains three highly conserved residues, Glu186, His380 and His400, as motifs A, B and C of the β-CASP family, respectively, in addition to four motifs (1 to 4) characteristic of metallo-β-lactamases. The presence of His as motif C is considered as a hallmark of specificity for RNA substrates (*6*). This configuration in the sequence predicted TTHA0252 to be a member of the β-CASP family involved in RNA metabolism.

Biophysical Properties—To investigate the activity of TTHA0252, the gene was engineered for heterologous expression in *E. coli* and the recombinant enzyme was purified in homogeneity. Size exclusion chromatography of the purified protein showed it to elute as a single peak with an apparent molecular mass of approximately 54 kDa (data not shown). This suggests that TTHA0252, with a calculated molecular mass of 47,055 Da, exists as a monomer in solution. Far-UV CD spectra showed negative maxima at 208 and 222 nm, indicating that the enzyme contains helical structures. Based on the dependence of the ellipticity at 222 nm, this protein was stable up to approximately 90°C at pH 7.0 (data not shown). The presence of zinc ions in the purified TTHA0252 was revealed by XAFS experiment. The stoichiometry of zinc binding to the purified protein was determined to be 0.7 mol of Zn per mol of protein by the PAR assay. This seemed to reflect weak binding of zinc ions to the protein since metallo-β-lactamases generally require two zinc ions per active site for catalysis (*22*).

Nuclease Activity—TTHA0252 exhibited nuclease activity against 23S and 16S rRNA of *T. thermophilus* HB8 (Fig. 2A). It showed no activity against short RNAs from *E. coli* (data not shown). Significant enzyme activity was observed without the incorporation of metal ions into the assay mix. In the absence of the protein, addition of zinc ion at low concentration, comparable to that of the protein assayed (5 μM), resulted in no rRNA degradation, although addition of zinc ions at higher concentrations (5 mM) caused degradation of rRNA even without the protein (data not shown). Cd^{2+}, Co^{2+}, Mn^{2+}, Ca^{2+}, Mg^{2+} or Ni^{2+} inhibited the enzyme activity to various degrees. Degradation of rRNA proceeded with time (Fig. 2C) and depended on enzyme concentration (Fig. 2D).

TTHA0252 showed no activity against DNA (Fig. 2B) and seemed to have no nicking or exonuclease activity against circular and linearized plasmid DNA. These results are in agreement with the predicted activity based on the residue of motif C.

Overall Structure—The crystal structure of TTHA0252 was solved by the SAD method using a SeMet derivative at a resolution of 2.8 Å (Fig. 3A). The overall structure of TTHA0252 consists of two domains. One domain (β-lactamase domain) containing both termini (residues 1–194 and 378–431) has a four-layered β-sandwich fold with two mixed β-sheets flanked by α-helices, which is similar to archetypal metallo-β-lactamases such as the enzyme from *Stenotrophomonas maltophilia* (*23*) (Fig. 3D). The metal-binding site is located at one edge of the β-sandwich. The other domain (residues 195–377) consists of α-helices and β-sheets. To obtain some clues about the possible function, the DALI search (*24*) for similar structures to this domain was performed. The result revealed similarity to EF2904 (described below) and several helicases and helicase-related proteins, such as Hef helicase (PDB code 1WP9), transcription-repair coupling factor (2EYQ), UvrB protein (1D2M) and RecQ helicase (1OYW), showed a Z-score above 7.0 and an r.m.s.d. below 3.5 Å. Such high Z-scores indicate the significance of the observed similarity, although no experimental data support this similarity. The cleft, with a width of at most 10 Å, is formed between the β-lactamase and the other domains (Fig. 3F). Since the metal-binding site is considered to be the active site, it is proposed that the substrate-binding site is located within the cleft. The width of the cleft suggests that TTHA0252 can recognize a single-stranded region, but not a double-stranded region (diameter ~20 Å), of RNA as substrate.

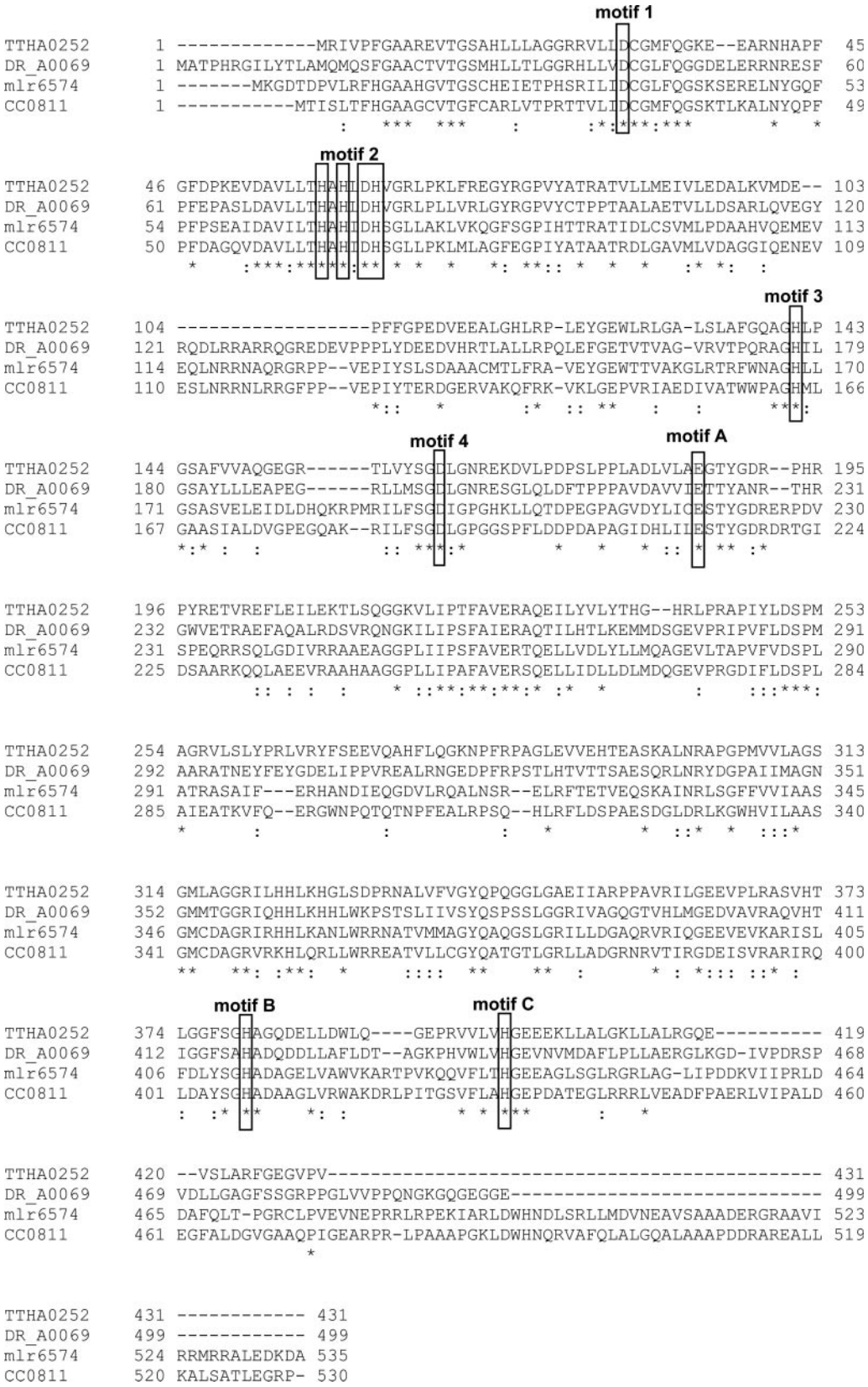

Fig. 1. **Alignment of β-CASP protein sequences.** Amino acid sequences are from *T. thermophilus* HB8 (TTHA0252), *Deinococcus radiodurans* (DR_A0069), *Mesorhizobium loti* (mlr6574) and *Caulobacter crescentus* (CC0811). The amino acid sequences were aligned using the program ClustalW (*26*). Completely and highly conserved residues are indicated by asterisks and colons.

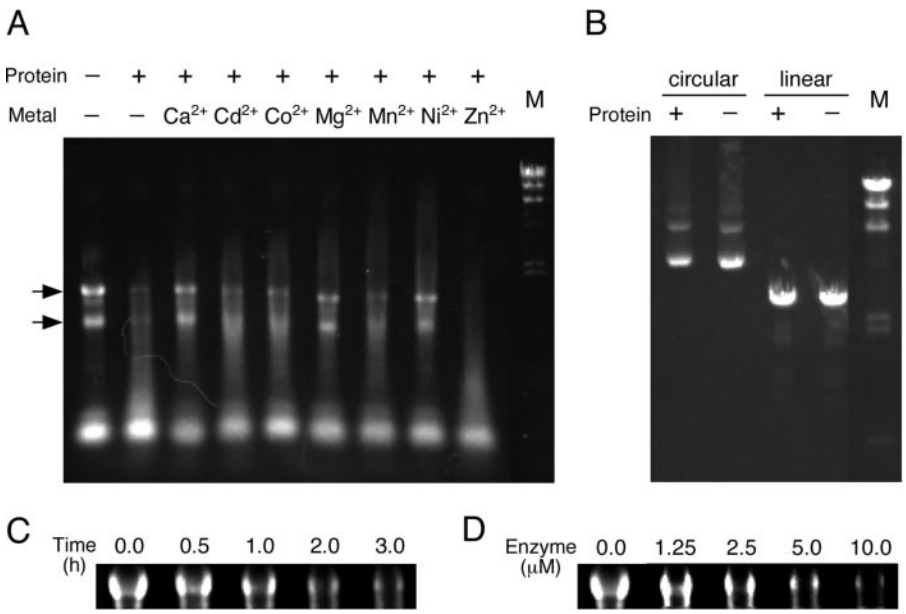

Fig. 2. **Nuclease activity of TTHA0252.** (A) Assay against *T. thermophilus* total RNA. Conditions for measurements are described in "EXPERIMENTAL PROCEDURES." Arrows indicate the positions of 23S and 16S rRNA. (B) Assay against DNA. Substrates are: circular, closed circular plasmid; linear, linearized plasmid. M, λ-*Hin*dIII digest. (C) Time-course of the activity. (D) Dependence of the activity on enzyme concentration. In (D), the reactions with 0, 1.25, 2.5, 5, 10 μM TTHA0252 were performed for 3 h.

This is the first report of the crystal structure of the β-CASP family protein and has revealed the configuration of the conserved residues in the predicted β-CASP domain. Contrary to prediction (*6*), the region ranging from motif A to motif C does not constitute a separate domain. Motif A (177–240) and motifs B-C (370–403) are remote from one another and present across the two domains. Pfam analysis assigned residues 13–223 and 363–404 as a metallo-β-lactamase fold and RMMBL fold, respectively. The RMMBL motif represents the fifth motif from metallo-β-lactamases involved in RNA metabolism, but contains only motifs B and C proposed by Callebaut *et al.* (*6*). The structure of TTHA0252 suggests that the β-CASP motif should be considered a characteristic feature of a RNA/DNA-metabolizing metallo-β-lactamase, but does not necessarily correspond to a separate domain in structure.

A structural similarity search using DALI (*24*) revealed the overall architecture of TTHA0252 shares a common fold with that of EF2904 from *Enterococcus faecalis* (Z = 24.0, PDB code 2AZ4), which is annotated as a hypothetical protein (Fig. 3E). Pfam analysis of EF2904 indicates that the sequence does not belong to any protein family including metallo-β-lactamase. Despite the low level of sequence identity between TTHA0252 and EF2904 (17%), the two proteins can be structurally aligned with an r.m.s.d. of 3.3 Å for 318 Cα atoms. The crystal structures of RNase Z, tRNA maturase, have been determined from *B. subtilis* (*8*, *9*) and *T. maritima* (*10*), but structural similarity with TTHA0252 is only observed in the β-lactamase domain. Therefore, the other domain of TTHA0252 is presumably responsible for the inherent properties of this enzyme. Based on the structural features of this domain, we named it the "clamp" domain.

Active Site—The putative active site of TTHA0252 comprises two zinc ions and residues from motifs 1–4 in the metallo-β-lactamase fold and motifs B-C in the RMMBL fold (Figs. 3B and 4A). The native crystal had an absorption edge at 1.2826 Å, which was similar to that of the zinc ion (1.2834 Å). The site of the zinc ions was confirmed by anomalous difference Fourier map using SAD data (Fig. 3C). The relatively weak electron density for both zinc ions is probably due to a low level of occupancy. Indeed, the relative occupancies of the two zinc ions estimated from the anomalous signals were 0.49 and 0.62. This is also consistent with the result of the PAR assay.

The zinc ions are coordinated by at least seven residues: one by His59 (motif 2), His61 (motif 2) and His 141 (motif 3), the other by Asp63 (motif 2), His64 (motif 2) and His400 (motif C), and both by Asp162 (motif 4) (Figs. 4A and 4C). No water molecule was found in this site. His380 and His 400 in the RMMBL motif form one side of the active site pocket in addition to Asp162 in motif 4, whereas three His and two Asp residues from the β-lactamase motif form the other side. Such a configuration is similar to those of archetypal metallo-β-lactamases (Fig. 4B). It is intriguing that His400, characteristic of the β-CASP family, structurally substitutes for the conserved histidine (His225 in Fig. 4B) in motif 5 of archetypal metallo-β-lactamases. The aspartic acid residues in motif 1 (Asp29/Asp37 in Fig. 4A/4B) and motif 4 (Asp162/Asp184) are located at equivalent positions in the respective active sites. Asp29 seems to stabilize His64 by formation of a hydrogen bond. Glu186 and His380 may stabilize His380 and Asp162, respectively, in a similar way to Asp29.

DISCUSSION

Some members of the β-CASP family may possess a similar biological role to that of *E. coli* RNase E, because *B. subtilis* RNase J1 and J2 both cleave the single-stranded region of

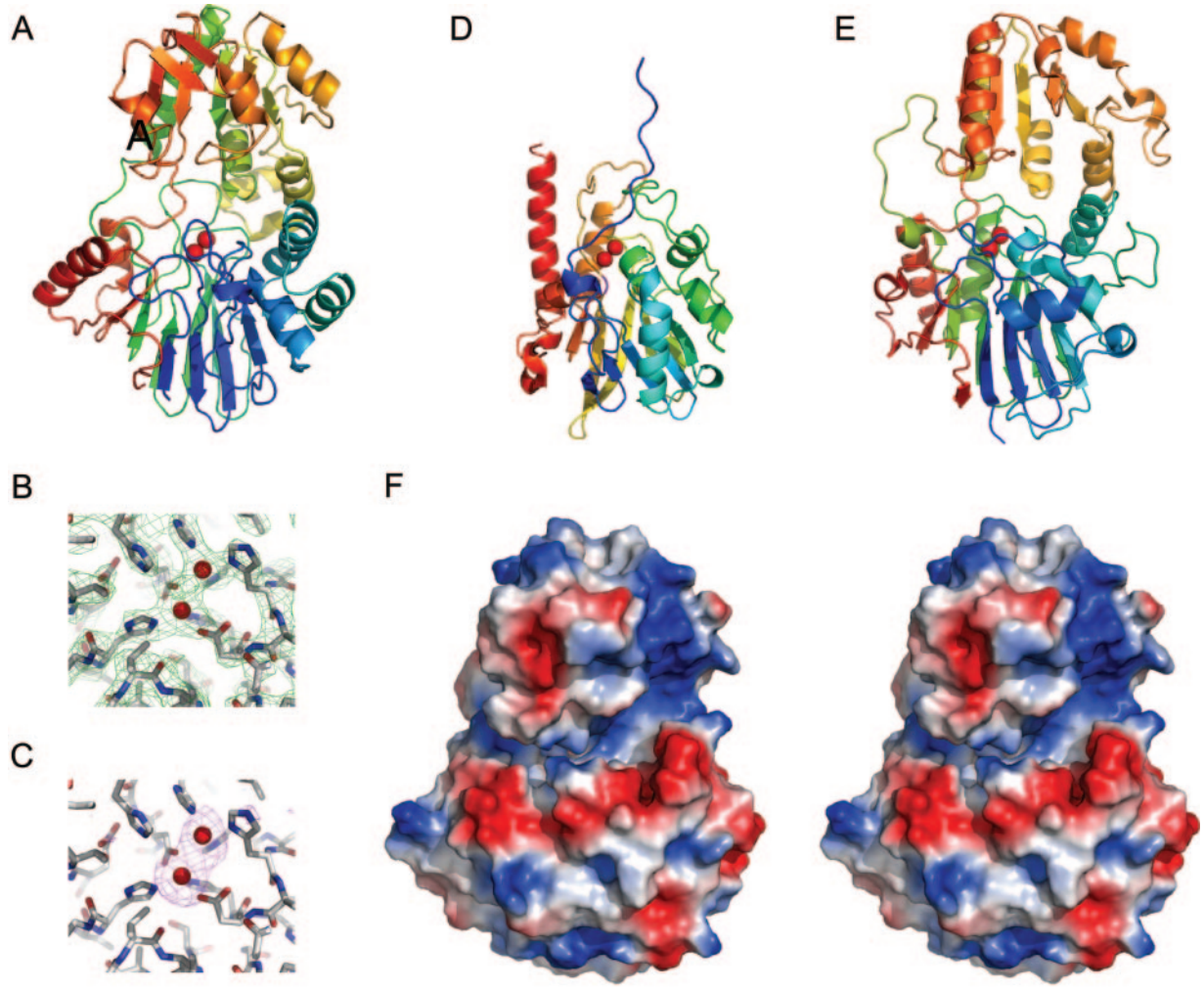

Fig. 3. **Crystal structure of TTHA0252.** (A) Overall structure of TTHA0252. (B) Active site of TTHA0252 with $2F_o$-F_c map at 1.5σ above the mean. (C) Active site of TTHA0252 with anomalous difference Fourier map (using the data at 1.2826 Å) at 3σ above the mean. These maps are shown superimposed on a molecular model. (D) *S. maltophilia* metallo-β-lactamase (PDB code 1SML). (E) *E. faecali* EF2904 (PDB code 2AZ4). Red spheres represent zinc ions. (F) Stereo view of the electrostatic potential map of TTHA0252.

the *thr*S mRNA leader at the same sites as RNase E (*5*). RNase E initiates mRNA decay by endonucleolytic cleavage, and is also important for maturation of 16S and 5S rRNAs (*2*). The observation that TTHA0252 degrades 23S and 16S rRNAs supports the notion that this enzyme is functionally homologous to *E. coli* RNase E. Furthermore, we could not find a homologue to *E. coli* RNase E in the *T. thermophilus* HB8 genome. The specific cleavage sites by RNase E and RNases J1/J2 were upstream of the terminator, which forms a stable secondary structure. These observations suggest that substrates for TTHA0252 are RNAs including secondary structures, such as loops and hairpins.

The crystal structure of TTHA0252 provides a structural basis for the substrate recognition. The overall structure is the first example of a metallo-β-lactamase superfamily protein with an architecture consisting of two distinct domains. Since the cleft between two domains contains the putative active site, we speculate that the clamp domain comprises the substrate-binding site. The dimension of the cleft suggests that the candidate for the molecule binding to the cleft is a single-stranded RNA. As mentioned above, however, the substrate RNA was assumed to contain secondary structures. This apparent discrepancy can be explained by proposing that the enzyme has an additional site for recognizing RNA secondary structures. It is unlikely that the β-lactamase domain is primarily responsible for this recognition. A positively charged area on the surface of the clamp domain adjacent to the cleft region of TTHA0252 (Fig. 3F) may play an important role in substrate specificity *via* interactions with the RNA molecule outside the cleavage site. This notion is consistent with the variation in length of the region between the motif 4 and the RMMBL motif among β-CASP family proteins. Dimeric RNase ZS (a short form), another metallo-β-lactamase superfamily protein, has a flexible arm (exocite module) that interacts with the tRNA molecule, although in this case the arm

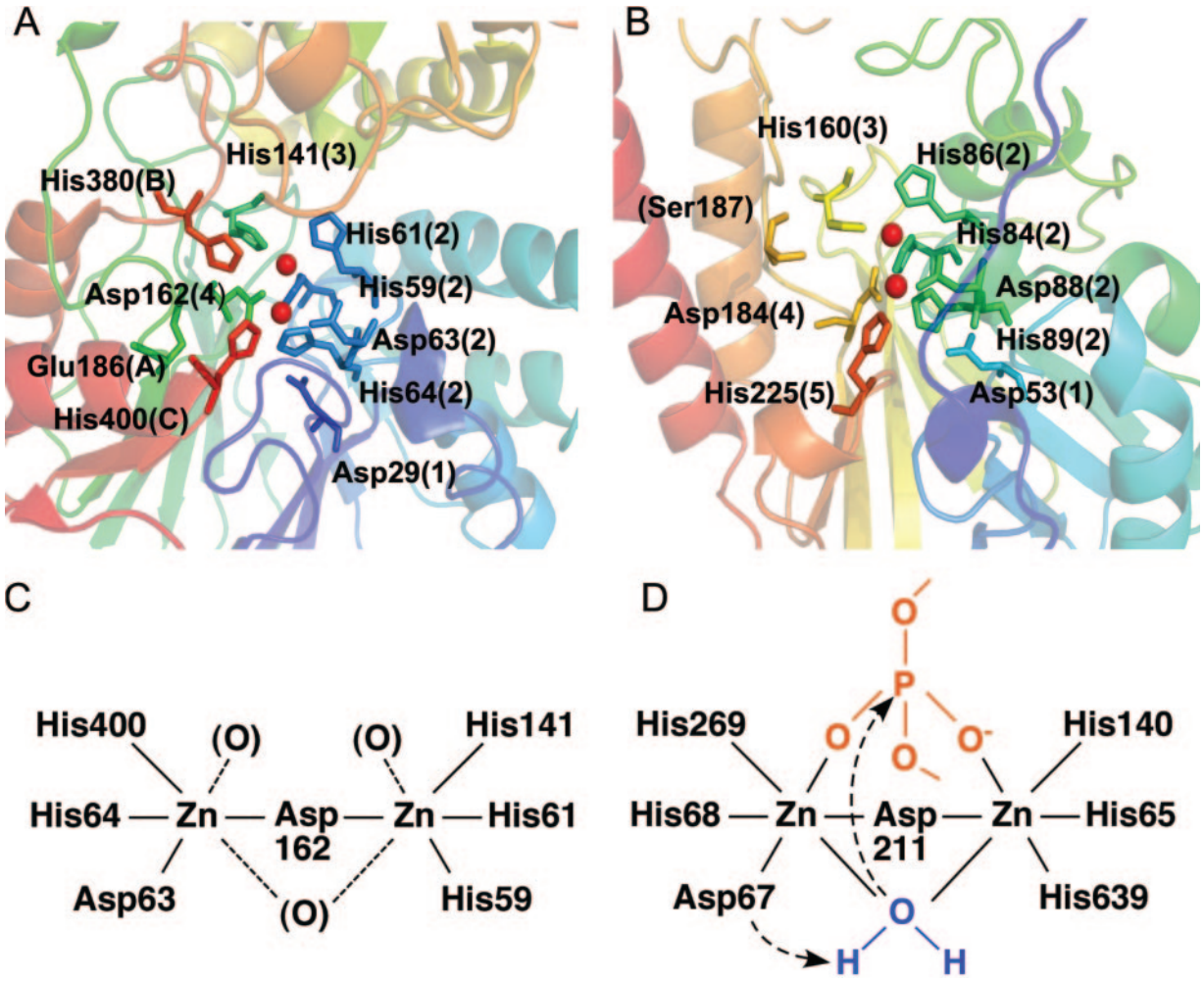

Fig. 4. **Comparison of the active site between TTHA0252 and other metallo-β-lactamase superfamily proteins.** (A) TTHA0252, (B) *S. maltophilia* metallo-β-lactamase (PDB code, 1SML). Red spheres indicate zinc ions. Numbers or letters in parentheses represent the names of the motifs. (C) Schematic structure of the active site of TTHA0252. Putative water molecules, unidentified in the TTHA0252 structure, are depicted as (O) at the positions by analogy with those in EF2904. (D) Schematic structure of the active site of *B. subtilis* RNase Z (*8*).

protrudes from the opposite side to the active site (*9*). RNase ZL (a long form) has an additional N-terminal extension, which might be involved in substrate recognition (*25*). RNases belonging to the metallo-β-lactamase superfamily may share a common architecture, in which additional features outside the metallo-β-lactamase domain participate in substrate recognition. The partial similarity between the clamp domain and helicases may support the notion that the clamp domain is involved in substrate RNA recognition.

The structure of TTHA0252 provides clues to the role of the motifs characteristic of the β-CASP family. Previously, the residue in motif C was hypothesized to be involved in substrate specificity (*i.e.* discrimination of RNA from DNA or β-lactams) (*6*). Our results suggest this hypothesis is unlikely, although no structure for the enzyme-substrate complex is available. The key finding is that His400 in motif C is coordinated to the zinc ion in place of the conserved His in motif 5 of other metallo-β-lactamases. Conservation of the histidine residue at this position indicates its essential role in catalysis. His380 in motif B may fix the active site pocket *via* interaction with Asp162 in motif 4. Otherwise, His380 may act as a ligand to a zinc ion indirectly through a hydrogen-bonded water molecule in a similar way to Ser187 of *S. maltophilia* L1 metallo-β-lactamase. Glu186 in motif A might also have a similar role by interacting with His380 or acting as a ligand indirectly.

Structural similarities between the active sites of TTHA0252 and EF2904 help to infer a putative coordination geometry of the zinc ions because the latter structure (at 2.0 Å resolution) contained water molecules in the active site. In EF2904, three water molecules liganded to the zinc ions permit for octahedral coordination. We here assume that both zinc sites of TTHA0252 have octahedral coordination similar to those of EF2904 (Fig. 4C). Such a geometry is similar to that in the active site of *B. subtilis* RNase Z, which has oxygen atoms from the backbone of the bound RNA as ligands to zinc ions (Fig. 4D). These similarities suggest these enzymes share a common catalytic mechanism. On this basis we can propose a mechanism for the cleavage reaction. The zinc ions exhibit octahedral coordination *via* the conserved His and Asp, an

unidentified water molecule, and the phosphate group of the bound RNA. Thus the phosphate group of the substrate is polarized by the two zinc ions, and the water molecule is activated by Asp63 (Asp67 in RNase Z) as a general base. The resultant hydroxide ion undergoes a nucleophilic attack on the phosphorus atom leading to phosphodiester bond cleavage.

This is the first reported crystal structure of a protein from the β-CASP family. The data will shed new light on the structural aspects of other β-CASP family proteins, such as human Artemis and yeast PSO2. From viewpoint of physiological aspect, TTHA0252 may form a large protein complex equivalent to the degradosome in *E. coli*, which includes RNase E, polynucleotide phosphorylase and DnaK. Further characterization of TTHA0252 is currently underway.

REFERENCES

1. Alberts, B., Bray, D., Lewis, J., Raff, M., Roberts, K., and Watson, J.D. (1999) *Molecular Biology of the Cell*, Garland Publishing, New York, NY
2. Deutscher, M.P. (2006) Degradation of RNA in bacteria: comparison of mRNA and stable RNA. *Nucleic Acids Res.* **34**, 659–666
3. Carpousis, A.J. (2002) The *Escherichia coli* RNA degradosome: structure, function and relationship in other ribonucleolytic multienzyme complexes. *Biochem. Soc. Trans.* **30**, 150–155
4. Kushner, S. (2002) mRNA decay in *Escherichia coli* comes of age. *J. Bacteriol.* **184**, 4658–4665
5. Even, S., Pellegrini, O., Zig, L., Labas, V., Vinh, J., Brechemmier-Baey, D., and Putzer, H. (2005) Ribonucleases J1 and J2: two novel endoribonucleases in *B. subtilis* with functional homology to *E. coli* RNase E. *Nucleic Acids Res.* **33**, 2141–2152
6. Callebaut, I., Moshous, D., Mornon, J.P., and de Villartay, J.P. (2002) Metallo-β-lactamase fold within nucleic acids processing enzymes: the β-CASP family. *Nucleic Acids Res.* **30**, 3592–3601
7. Aravind, L. (1999) An evolutionary classification of the metallo-β-lactamase fold proteins. *In Silico Biol.* **1**, 69–91
8. Li de la Sierra-Gallay, I., Pellegrini, O., and Condon, C. (2005) Structural basis for substrate binding, cleavage and allostery in the tRNA maturase RNase Z. *Nature* **433**, 657–661
9. Li de la Sierra-Gallay, I., Mathy, N., Pellegrini, O., and Condon, C. (2006) Structure of the ubiquitous 3′ processing enzyme RNase Z bound to transfer RNA. *Nat. Struct. Mol. Biol.* **13**, 376–377
10. Ishii, R., Minagawa, A., Takaku, H., Takagi, M., Nashimoto, M., and Yokoyama, S. (2005) Crystal structure of the tRNA 3′ processing endoribonuclease tRNase Z from *Thermotoga maritima*. *J. Biol. Chem.* **280**, 14138–14144
11. Oshima, T. and Imahori, K. (1974) Description of *Thermus thermophilus* comb. nov., a non-sporulating thermophilic bacterium from a Japanese thermal spa. *Int. J. Syst. Bacteriol.* **24**, 102–112
12. Yokoyama, S., Hirota, H., Kigawa, T., Yabuki, T., Shirouzu, M., Terada, T., Ito, Y., Matsuo, Y., Kuroda, Y., Nishimura, Y., Kyogoku, Y., Miki, K., Masui, R., and Kuramitsu, S. (2000) Structural genomics projects in Japan. *Nat. Struct. Biol.* **7(Suppl)**, 943–945
13. Sambrook, J. and Russel, D.W. (2001) *Molecular Cloning*, Cold Spring Harbor Laboratory Press, Cold Spring Harbor, NY
14. LeMaster, D.M. and Richards, F.M. (1985) ^{1}H-^{15}N heteronuclear NMR studies of *Escherichia coli* thioredoxin in samples isotopically labeled by residue type. *Biochemistry* **24**, 7263–7268.
15. Kuramitsu, S., Hiromi, K., Hayashi, H., Morino, Y., and Kagamiyama, H. (1990) Pre-steady-state kinetics of *Escherichia coli* aspartate aminotransferase catalyzed reactions and thermodynamic aspects of its substrate specificity. *Biochemistry* **29**, 5469–5476.
16. Otwinowski, Z. and Minor, W. (1997) Processing of X-ray diffraction data collected in oscillation mode. *Methods Enzymol.* **276**, 307–326
17. Collaborative Computational Project, number 4. (1994) The CCP4 suite: programs for protein crystallography. *Acta Crystallogr. D* **50**, 760–763
18. Terwilliger, T.C. and Berendzen, J. (1999) Automated MAD and MIR structure solution. *Acta Crystallogr. D* **55**, 849–861
19. Terwilliger, T.C. (2000) Maximum likelihood density modification. *Acta Crystallogr. D* **56**, 965–972
20. McRee, D.E. (1999) XtalView/Xfit—A versatile program for manipulating atomic coordinates and electron density. *J. Struct. Biol.* **125**, 156–165
21. Brunger, A.T., Adams, P.D., Clore, G.M., DeLano, W.L., Gros, P., Grosse-Kunstleve, R.W., Jiang, J.S., Kuszewski, J., Nilges, M., Pannu, N.S., *et al.* (1998) Crystallography & NMR system: A new software suite for macromolecular structure determination. *Acta Crystallogr. D* **54**, 905–921
22. Wang, Z., Fast, W., Valentine, A.M., and Benkovic, S.J. (1999) Metallo-β-lactamase: structure and mechanism. *Curr. Opin. Chem. Biol.* **3**, 614–622
23. Ullah, J.H., Walsh, T.R., Taylor, I.A., Emery, D.C., Verma, C.S., Gamblin, S.J., and Spencer, J. (1998) The crystal structure of the L1 metallo-beta-lactamase from *Stenotrophomonas maltophilia* at 1.7 Å resolution. *J. Mol. Biol.* **284**, 125–136
24. Holm, L. and Sander, C. (1999) Protein folds and families: sequence and structure alignments. *Nucleic Acids Res.* **27**, 244–247
25. Takaku, H., Minagawa, A., Takagi, M., and Nashimoto, M. (2004) The N-terminal half-domain of the long form of tRNase Z is required for the RNase 65 activity. *Nucleic Acids Res.* **32**, 4429–4438
26. Higgins, D., Thompson, J., Gibson, T., Thompson, J.D., Higgins, D.G., and Gibson, T.J. (1994) CLUSTAL W: improving the sensitivity of progressive multiple sequence alignment through sequence weighting, position-specific gap penalties and weight matrix choice. *Nucleic Acids Res.* **22**, 4673–4680